



THIS MANUSCRIPT HAS BEEN SUBMITTED TO THE JOURNAL OF GLACIOLOGY AND HAS NOT BEEN PEER-REVIEWED.

Simulating Seasonal Evolution of Subglacial Hydrology at a Surging Glacier in the Karakoram

Journal:	<i>Journal of Glaciology</i>
Manuscript ID	Draft
Manuscript Type:	Article
Date Submitted by the Author:	n/a
Complete List of Authors:	Narayanan, Neosha; Georgia Institute of Technology, ; Massachusetts Institute of Technology, Sommers, Aleah; Dartmouth College, Thayer School of Engineering Chu, Winnie; Georgia Institute of Technology Steiner, Jakob; University of Graz Faculty of Natural Sciences, Siddique, Muhammad; Information Technology University Meyer, Colin; Dartmouth College, Thayer School of Engineering Minchow, Brent; Massachusetts Institute of Technology, Department of Earth, Atmospheric and Planetary Sciences
Keywords:	Glacier surges, Subglacial processes, Glacier modelling, Mountain glaciers
Abstract:	Glacier motion, retreat, and glacier hazards such as surges and glacial lake outburst floods (GLOFs) are likely underpinned by subglacial hydrology. Recent advances in subglacial hydrological modeling allow us to shed light on subglacial processes that lead to changes in ice mass balance and GLOFs in High Mountain Asia (HMA). We present the first application of the SHAKTI subglacial hydrology model on an alpine glacier. Shishper Glacier, our study site, is a surge-type glacier in northern Pakistan that exhibits concurrent GLOFs which endanger local communities and infrastructure. The subglacial hydrological system undergoes transitions between inefficient to efficient drainage and back during spring and fall, supporting previous observations of spring and fall speedups of glaciers in the region. We also conclude that subglacial hydrology, while important in sliding dynamics, cannot provide a

	<p>standalone explanation for surging, implicating a need for coupled hydrological and ice dynamics modeling of surge conditions. This work demonstrates the potential of using ice sheet models for alpine glaciology and provides a new nucleus for modeling of glacial hazards in alpine environments.</p>

SCHOLARONE™
Manuscripts

1 Simulating Seasonal Evolution of Subglacial Hydrology at a 2 Surging Glacier in the Karakoram

3 Neosha NARAYANAN,^{1,2} Aleah SOMMERS,³ Winnie CHU,¹ Jakob STEINER,^{4,5} Muhammad
4 Adnan SIDDIQUE,⁶ Colin R MEYER,³ Brent MINCHEW²

5 ¹ *Georgia Institute of Technology, Department of Earth and Atmospheric Sciences, Atlanta, GA, USA*

6 ² *Massachusetts Institute of Technology, Department of Earth, Atmospheric, and Planetary Sciences,
7 Cambridge, MA, USA*

8 ³ *Dartmouth College, Thayer School of Engineering, Hanover, NH, USA*

9 ⁴ *Himalayan University Consortium, Lalitpur, Nepal*

10 ⁵ *Institute of Geography and Regional Science, University of Graz, Austria*

11 ⁶ *Information Technology University, Lahore, Pakistan*

12 *Correspondence: Neosha Narayanan <nnarayanan38@gatech.edu>*

13 **ABSTRACT.**

14 **Glacier motion, retreat, and glacier hazards such as surges and glacial lake**
15 **outburst floods (GLOFs) are likely underpinned by subglacial hydrology. Re-**
16 **cent advances in subglacial hydrological modeling allow us to shed light on sub-**
17 **glacial processes that lead to changes in ice mass balance and GLOFs in High**
18 **Mountain Asia (HMA). We present the first application of the SHAKTI sub-**
19 **glacial hydrology model on an alpine glacier. Shishper Glacier, our study site,**
20 **is a surge-type glacier in northern Pakistan that exhibits concurrent GLOFs**
21 **which endanger local communities and infrastructure. The subglacial hydro-**
22 **logical system undergoes transitions between inefficient to efficient drainage**
23 **and back during spring and fall, supporting previous observations of spring**
24 **and fall speedups of glaciers in the region. We also conclude that subglacial**
25 **hydrology, while important in sliding dynamics, cannot provide a standalone**
26 **explanation for surging, implicating a need for coupled hydrological and ice**
27 **dynamics modeling of surge conditions. This work demonstrates the potential**

28 **of using ice sheet models for alpine glaciology and provides a new nucleus for**
29 **modeling of glacial hazards in alpine environments.**

30 INTRODUCTION

31 The High Mountain Asia (HMA) region, known as the “Third Pole,” contains the largest concentration of
32 ice outside of the polar ice sheets. The glaciers of HMA feed major water systems which provide water
33 and sanitation for over a billion people (Scott and others, 2019). In particular, the Karakoram is the
34 most heavily glaciated mountain range in Asia (RGI Consortium, 2017) and is a critical water source for
35 large parts of Pakistan and parts of northern India (Scott and others, 2019). However, climate change
36 has led to increasingly negative mass balance, putting the area’s future at risk (Zhang and others, 2023a;
37 Shean and others, 2020; Rounce and others, 2020; Bolch and others, 2011). Glacial lake outburst floods
38 (GLOFs) in the region have also caused significant loss of human lives and infrastructure damage in recent
39 decades (Shrestha and others, 2023), and the risk of exposure to local communities and infrastructure due
40 to growing proglacial lakes may potentially increase (Zhang and others, 2023b, 2024; Zheng and others,
41 2021; Harrison and others, 2018). GLOFs in the Karakoram region occur through breaches of moraine or
42 ice dams, which are associated with rapid (re)-organization of subglacial waters and channels (Nye, 1976;
43 Gudmundsson and others, 1995; Bigelow and others, 2020; Kingslake and Ng, 2013; Flowers and others,
44 2004). Proglacial and proximal lakes, which are often hydraulically connected with the subglacial drainage
45 network, also exert an important boundary condition on the subglacial water network (Bigelow and others,
46 2020; Anderson and others, 2005; Armstrong and Anderson, 2020)).

47 The Karakoram region is also home to a high concentration of surge-type glaciers (Sevestre and Benn,
48 2015; Copland and others, 2009, 2011). Surges are a phenomenon characterized by cyclical, order-of-
49 magnitude accelerations of glaciers that can be sustained for months to years (Eisen and others, 2001; Jay-
50 Allemand and others, 2011; Round and others, 2017; Bhambri and others, 2020; Björnsson, 1998). They
51 occur in geographical clusters that fall in “climatic envelopes” that may provide favorable temperatures
52 and accumulation rates for surge motion (Sevestre and Benn, 2015; Jiskoot and others, 2000). Surges are
53 also associated with till deformation (Minchew and Meyer, 2020; Minchew and others, 2016). Buildups
54 of basal water pressure are thought to play a role in the initiation and sustenance of surge motion (e.g.,
55 Kamb (1987); Flowers and others (2011); Björnsson (1998); Jay-Allemand and others (2011)). However,

56 the causes of surge behavior remain unclear as not all surging glaciers seem to directly attributable to
57 changes in mass-balance state or thermal regime (e.g., Liu and others (2024); Murray and others (2000)).

58 Subglacial hydrology controls ice velocity through changes in effective pressure, defined as the difference
59 between the overburden pressure and the hydraulic head at the bed (Nienow and others, 2005). Seasonal
60 variations in subglacial hydrology modulate ice sheet and glacier velocities in Iceland and Greenland (Hart
61 and others, 2022; Sommers and others, 2024; Schoof, 2010; Zwally and others, 2002; Iken and others, 1983).
62 Numerous studies have shown that the velocity of glaciers increases during melt seasons (e.g., Nanni and
63 others (2023); Zwally and others (2002); Hart and others (2022); Bhambri and others (2020)). In alpine
64 glaciers of HMA, observed regional speedups have been proposed to occur due to changes in subglacial
65 drainage efficiency. In particular, these glaciers can also exhibit a pattern of speedups in both the spring
66 and fall (Beaud and others, 2022; Nanni and others, 2023). It is inferred that these seasonal speedups
67 occur due to variations in meltwater production and subsequent lubrication at the ice-bed interface.

68 While surges and outburst flooding have for the most part been investigated as separate phenomena,
69 multiple studies in the Karakoram have observed GLOFs to occur concurrently with transitions in surge
70 motion, suggesting that subglacial hydrology may play a non-straightforward role in the synchronous timing
71 of these events (Beaud and others, 2021; Bhambri and others, 2020; Bazai and others, 2022a; Round and
72 others, 2017; Bazai and others, 2022b; Steiner and others, 2018). Understanding the role that subglacial
73 hydrology plays in the severity and timing of these hazards could improve early warning systems for water
74 availability and outburst flooding. While several in-situ observational studies have been conducted and are
75 in progress (e.g., Gilbert and others (2020); Miles and others (2021, 2019); Pritchard and others (2020))
76 there are very few direct observations of subglacial hydrology in HMA. Therefore, in this study, we lay
77 the groundwork for investigating the role of subglacial hydrology in ice dynamics and outburst flooding
78 through modeling.

79 We focus on Shishper Glacier (36.40°N 74.61°E) in the eastern Karakoram range in Pakistan (Fig. 1).
80 The glacier has also been referred to in literature as Shisper and Shishpare. Located in the Hunza Valley
81 in Gilgit-Baltistan, Pakistan, Shishper is part of a surge and lake drainage system with another glacier
82 to its west, called Muchuwar (also previously spelled as Muchuhar or Mochowar). The two glaciers were
83 connected prior to 1950, when the two separated (Muhammad and others, 2021). Shishper's main trunk
84 is approximately 7 km long and is fed by several tributary glaciers at the northeast (upper-elevation) side.
85 In total, the glacier is about 15 km in length.

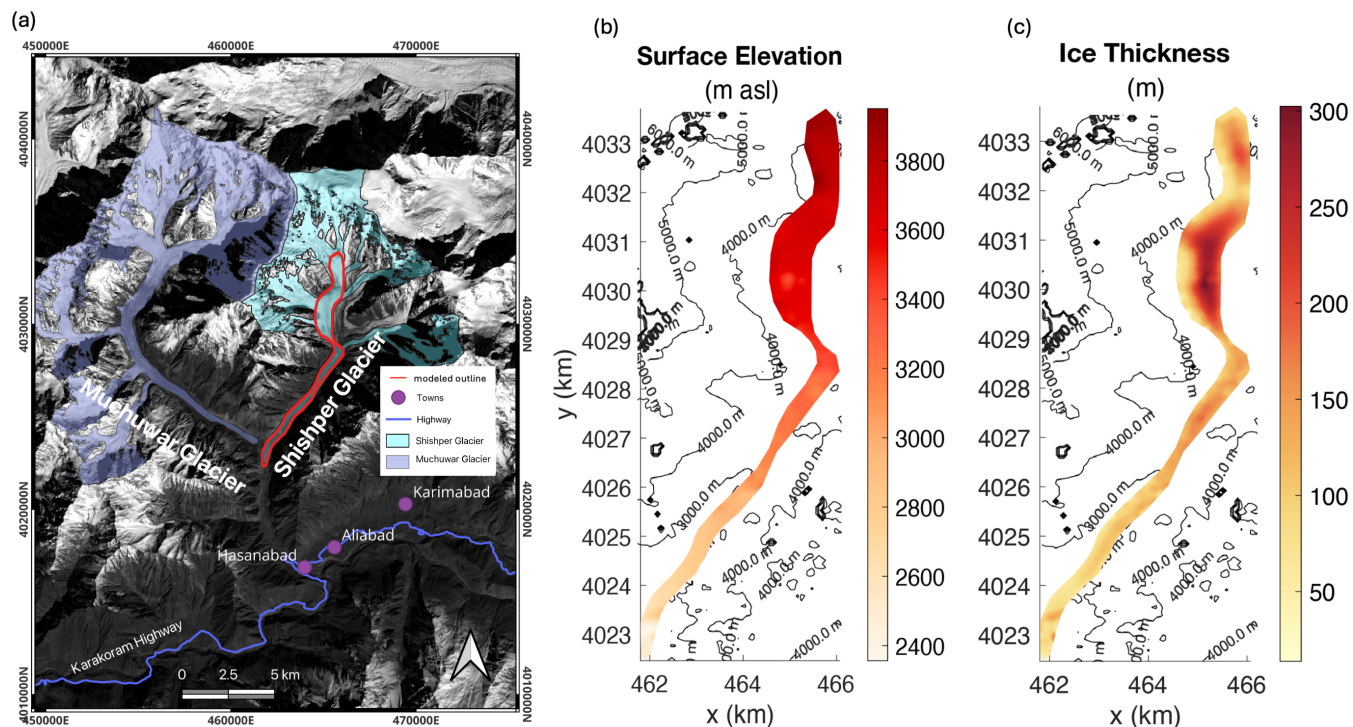


Fig. 1. (a) Outlines of adjacent valley glaciers Shishper and Muchuwar (Randolph Glacier Inventory Version 6.0) overlaid on Landsat 8 OLI NIR imagery from December 2016. Our modeled domain is outlined in red. (b) Surface elevation from TanDEM-X 90m DEM. (c) Ice thickness from Millan and others (2022)'s global dataset.

86 Both Shishper and Muchuwar have surged cyclically for as long as observations have been recorded,
 87 since the early 1900s (Beaud and others, 2021). Shishper underwent major surges in 1973, 2000-2011 and
 88 most recently between 2017-2019 (Bhambri and others, 2020). During this time, the terminus advanced
 89 approximately 1.5 km (Bhambri and others, 2020). In 2019, the surge and resulting lake drainage resulted in
 90 the closing of two power plants, the evacuation and considerable damage of some houses in the downstream
 91 village, lasting damage to agricultural land, and finally the destruction of the main road bridge crossing
 92 the stream, affecting transport along the main transport axis in the region. In mid-November 2018, the
 93 advancement of Shishper blocked meltwater flow from Muchuwar Glacier, which created an ice-dammed
 94 proximal lake (Beaud and others, 2022). This lake tends to fill up in November-December and in May to
 95 a depth of 30-80m, with an estimated volume of 30 million m^3 . When the lake drains, the outburst flood
 96 drains through the terminus of Shishper and down into the valley below. The maximum river flow observed
 97 at the downstream village of Hassanabad is $150\text{-}200 \text{ m}^3 \text{ s}^{-1}$, compared to a base flow of about $20 \text{ m}^3 \text{ s}^{-1}$
 98 (Muhammad and others, 2021). After the lake is filled in the winter, drainage occurs more gradually, as
 99 opposed to the spring filling which results in a more dramatic drainage of the lake.

100 In this study, we simulate the seasonal dynamics of the subglacial drainage system of Shishper Glacier.

101 We use a state-of-the-art subglacial hydrology model, forced with realistic meltwater inputs, to gain insight
102 into the evolution of the water flow and pressure distribution beneath the glacier. The following sections
103 describe the modeling methods and assumptions, meltwater forcing data, simulation results, a discussion
104 of implications for understanding surge initiation and cessation, and limitations of the approach.

105 **MODEL SETUP AND ASSUMPTIONS**

106 To simulate the subglacial hydrological system of Shishper Glacier, we employ the SHAKTI (Subglacial
107 Hydrology and Kinetic, Transient Interactions) model (Sommers and others, 2018), which is implemented
108 in the Ice-sheet and Sea-level System Model (ISSM) (Larour and others, 2012). SHAKTI is capable of
109 modeling a variety of network systems between the end-member cases of efficient and inefficient drainage
110 systems. It does this by allowing the hydraulic transmissivity to vary spatially and temporally (Sommers
111 and others, 2018). In addition, it accounts for varying laminar, turbulent, and intermediate flow regimes
112 (Sommers and others, 2018).

113 The model domain is traced from the Randolph Glacier Inventory, Version 6.0 (RGI Consortium,
114 2017). The tributary branches of Shishper Glacier, located above 3500 m asl, likely experience less liquid
115 precipitation and decreased melting compared to the lower section of the main trunk and therefore may
116 not contribute as much to the subglacial hydrological system. Our aim is to examine the evolution in the
117 hydrology in the main trunk, rather than evaluating the exact quantity of subglacial water in the system;
118 for these reasons, we reserve including hydrological contributions from the tributary glaciers for future
119 work. The modeled hydrological domain overlaid on the RGI 6.0 outline is shown in Fig. 1. The outline is
120 from 2016, before the 2017-2019 surge event. We focus on modeling the subglacial hydrology and do not
121 change the glacier outline or ice thickness.

122 To obtain a geometry for the glacier, we use the TanDEM-X global DEM (German Aerospace Center,
123 2018) along with a global glacier thickness dataset (Millan and others, 2022). Glacier thickness is subtracted
124 from surface elevation to obtain a bed topography, and all spatial data are projected to WGS 84/UTM
125 Zone 42N. We manually trace the model domain to the RGI outline using in-built functionality in ISSM.
126 The DEM and bed topography data are interpolated onto a 2-dimensional unstructured triangular mesh
127 with 40 m resolution. This mesh size and geometry were determined after conducting a winter equilibration
128 for 600 days at varying mesh sizes (shown in Appendix A). We conclude from these tests that the location
129 of channel formations is insensitive to mesh size. The 40 m resolution provides enough detail and stability

130 while saving on computational costs. The mesh provides the basis for the P1 triangular Lagrange finite
131 element solver used by SHAKTI. To ensure model stability and robustness, we test 20 slightly varying
132 domain shapes and conduct a winter equilibration, wherein all subglacial water is generated by basal
133 melt (see section “Establishing Winter Base State”) for 1000 days on each. The final geometry used for
134 the transient simulations is chosen based on the criteria that mean gap height, basal flux, and effective
135 pressure equilibrate after 1000 days. Finally, the velocity boundary condition is set to 0 throughout all
136 of the transient simulations, allowing us to isolate the evolution of subglacial hydrology without frictional
137 heating feedbacks from basal sliding.

138 All simulations in this work are carried out with ISSM Version 4.23 using a MATLAB interface on
139 MacOS.

140 Surface Melt Timeseries

141 To estimate timing and magnitude of seasonal meltwater inputs to the bed, we used the European Centre for
142 Medium-Range Weather Forecasts (ECMWF)’s Reanalysis v5 (ERA5) (Muñoz-Sabater and others, 2021)
143 as inputs to Litt and others (2019)’s temperature-indexed ice melt model to obtain spatio-temporally
144 varying estimates for surface melt across the domain (Fig. 2). These ERA5 weather data are based on an
145 array of field stations and weather models (Setchell, 2020), and directly provide estimates for snow cover,
146 air temperature, and total liquid precipitation across the five years (Muñoz-Sabater and others, 2021).
147 Ice melt across the mesh is calculated using the temperature index (TI) melt parametrization from Litt
148 and others (2019) (Fig. 2). We calculate daily melt over ice when the glacier surface is bare (using a
149 temperature index of $6.5 \text{ mm } ^\circ\text{C}^{-1} \text{ day}^{-1}$, computed from values from Litt and others (2019) and melt
150 from snow for pixels that are snow covered (using an index of $4.1 \text{ mm } ^\circ\text{C}^{-1} \text{ day}^{-1}$, following Braithwaite
151 (2008)). While melt or surface runoff from rainfall from outside the model domain may also reach the
152 model domain and eventually the glacier bed, we do not consider these inputs here. The TI model is shown
153 to be more accurate for glaciers below 3500 m above sea level (a.s.l) (Litt and others, 2019), which is where
154 most of Shishper’s tongue is located (Fig. 1). The melt and liquid precipitation data was downscaled from
155 its native 9 km to the model resolution (50 m) using a Kriging interpolation (Kusch and Davy, 2022).
156 While some in-situ climate data is available in the region, no station was operational in the vicinity of the
157 glacier; using in-situ data from an off-glacier station far away from the glacier would introduce its own set
158 of uncertainties. Due to the relatively high temporal (1 day) and spatial (1 deg^2) resolutions, relying on

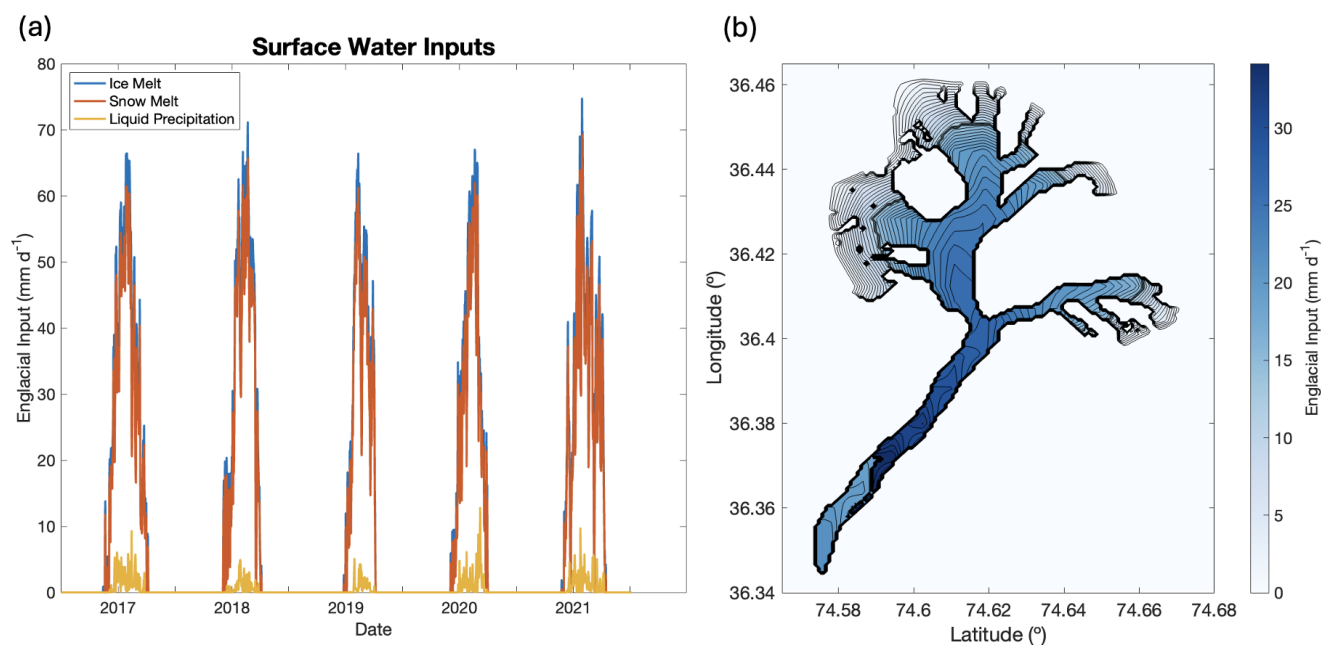


Fig. 2. (a) Englacial inputs to the transient subglacial hydrology model, averaged over the glacier, as calculated by ERA-5 Land and the temperature-indexed ablation model. (b) Average englacial input during the 2017 melt season (May through September).

159 ERA5 data is considered sufficient here.

160 The strong hydraulic coupling between surface and basal meltwater environments (Miles and others,
 161 2017; Zwally and others, 2002; Iken and Bindshadler, 1986; Shepherd and others, 2009; Gulley and Benn,
 162 2007) has given us justification to make the assumption that all meltwater inputs to the bed (i.e., surface
 163 melt, rainwater, aquifer contributions) are instantaneous. In reality, englacial water storage can delay the
 164 delivery of surface water to the base (Miles and others, 2017; Gulley and Benn, 2007); however, we neglect
 165 it in these simulations due to a lack of constrained knowledge about delay timing and storage magnitude.

166 TRANSIENT GLACIER HYDROLOGY SIMULATIONS

167 Establishing Winter Base State

168 Before transient simulations can be run, the base winter state of the hydrological system must be estab-
 169 lished. To do this, we prescribe some initial input parameters (Table 1) and allow the system to equilibrate.
 170 During the winter, we assume that there is no surface or englacial melt, with geothermal flux and melt
 171 opening/turbulent dissipation as the only hydrological inputs to the bed. Note that we have prescribed
 172 sliding velocity to be zero, so there is no frictional heating or cavity opening from sliding over bumps.

Table 1. Constants and parameter values used in this study

Symbol	Value	Units	Description
A	9.3×10^{-25}	$\text{Pa}^{-3} \text{s}^{-1}$	Flow law parameter
G	0.07	W m^{-2}	Geothermal flux
g	9.81	m s^{-2}	Gravitational acceleration
H	Varying	m	Ice thickness
L	3.34×10^5	J kg^{-1}	Latent heat of fusion of water
n	3	Dimensionless	Flow law exponent
z_b	Varying	m	Bed elevation with respect to sea level
ν	1.787×10^{-6}	$\text{m}^2 \text{s}^{-1}$	Kinematic viscosity of water
ω	0.001	Dimensionless	Parameter controlling nonlinear laminar/turbulent transition
ρ_i	917	kg m^{-3}	Bulk density of ice
ρ_w	1000	kg m^{-3}	Bulk density of water

173 Because we exclude all contributions from tributary glaciers, a Neumann boundary condition of zero flux
 174 is applied to all edges of the domain. A coarse time step of 1 day is sufficient for obtaining the final
 175 equilibrated state.

176 Once all output parameters reach equilibrium, after approximately 600 days, there is clear formation of
 177 a channel down the main trunk of the glacier (Fig. 3a). It is important to note that the channel has formed
 178 in the absence of any surface water melt, indicating its potential to persist through the winter months just
 179 given a small amount of geothermal heat flux and pressure melting. This perennial channel then forms the
 180 basis for the subglacial system during the melt season.

181 The subglacial drainage network reaches a second stable equilibrium following a year of transient sea-
 182 sonal melt forcing. Beginning from the base winter state (Fig. 3a), we run a transient simulation of 1 year
 183 (January 1 - December 31). Following this year, the model reaches a new stable winter state (Fig. 3b).
 184 The second stable state is largely similar to the first, but shows more efficient, concentrated drainage at
 185 a few isolated areas including the terminus and up-glacier at 4028 km N. Running additional melt sea-
 186 sons yields no additional changes in winter drainage patterns, indicating that this is a new equilibrium.
 187 The presence of this second equilibrium indicates that the cyclical melt season is necessary to maintain a
 188 perennial channel down the main trunk that returns to a similar configuration each winter.

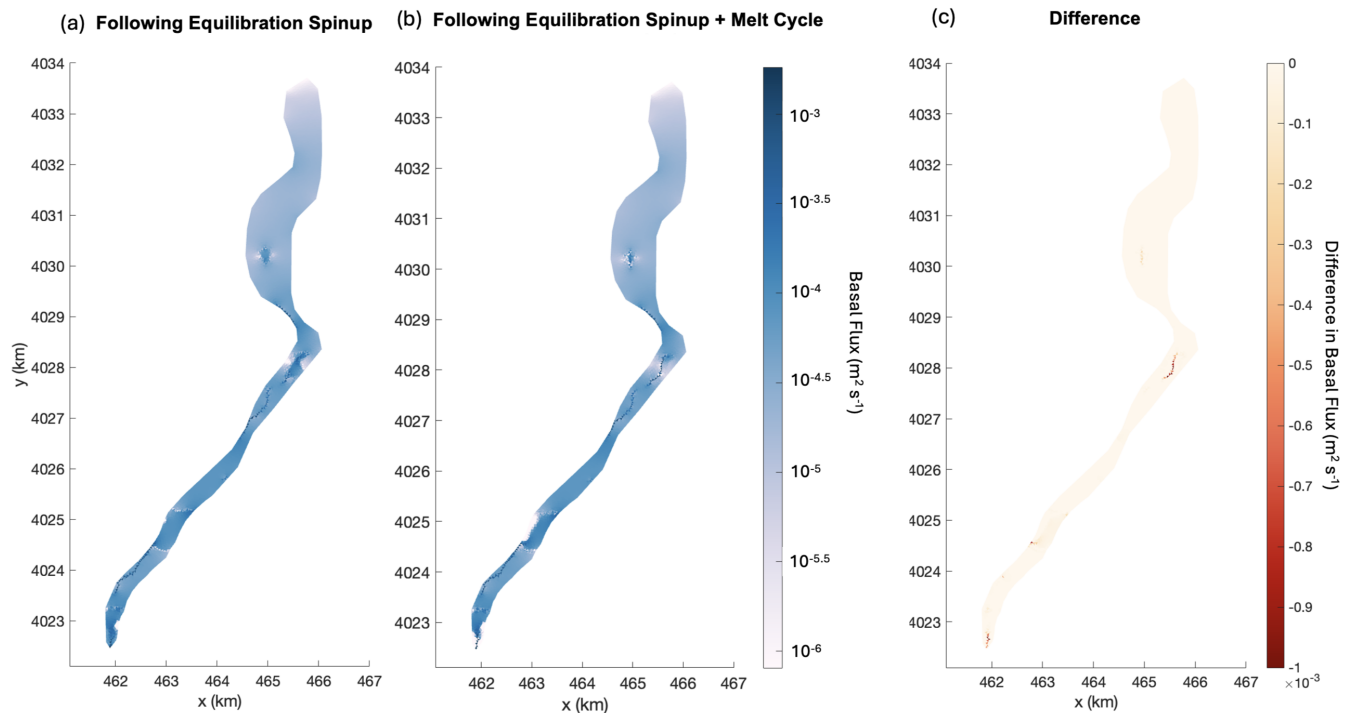


Fig. 3. Basal flux across the modeled domain following (a) a “winter state” equilibration spinup with no melt inputs to the system (b) a transient simulation through a full calendar year including a summer melt season and return back to frozen winter conditions. (c) The difference between the two equilibrated states.

189 Seasonal Evolution of Subglacial Hydrology

190 To understand how Shishper’s subglacial drainage network responds to seasonal changes in meltwater
 191 flux, we run transient simulations across a period of five years, 2017–2021. The transient input for these
 192 simulations is the temporally and spatially varying sum of ice melt, snow melt, and liquid precipitation
 193 (Fig. 2). Melt inputs from tributary glaciers are excluded from the simulations.

194 Fig. 4 illustrates changes in the configuration of the drainage system throughout 2017, which is repre-
 195 sentative of the pattern observed across all five years. We see a mostly closed system in winter (Fig. 4b)
 196 which transitions to a highly efficient, channelized system at the peak of the melt season (Fig. 4c). At the
 197 peak of the melt season, the drainage system extends to the northernmost part of the domain, splitting
 198 into arborescent patterns characteristic of channelized drainage (Röthlisberger, 1972). By October 5, these
 199 channels then disappear, with the upper part of the system having completely shut down. Finally, the
 200 system returns to the winter state by late October (Fig. 4d and e).

201 The lower channel which traverses the mid- to lower trunk clearly persists through every simulated
 202 winter in 2017–2021, and can be seen in both images of the “closed” state (Fig. 4a, d, and e). We know

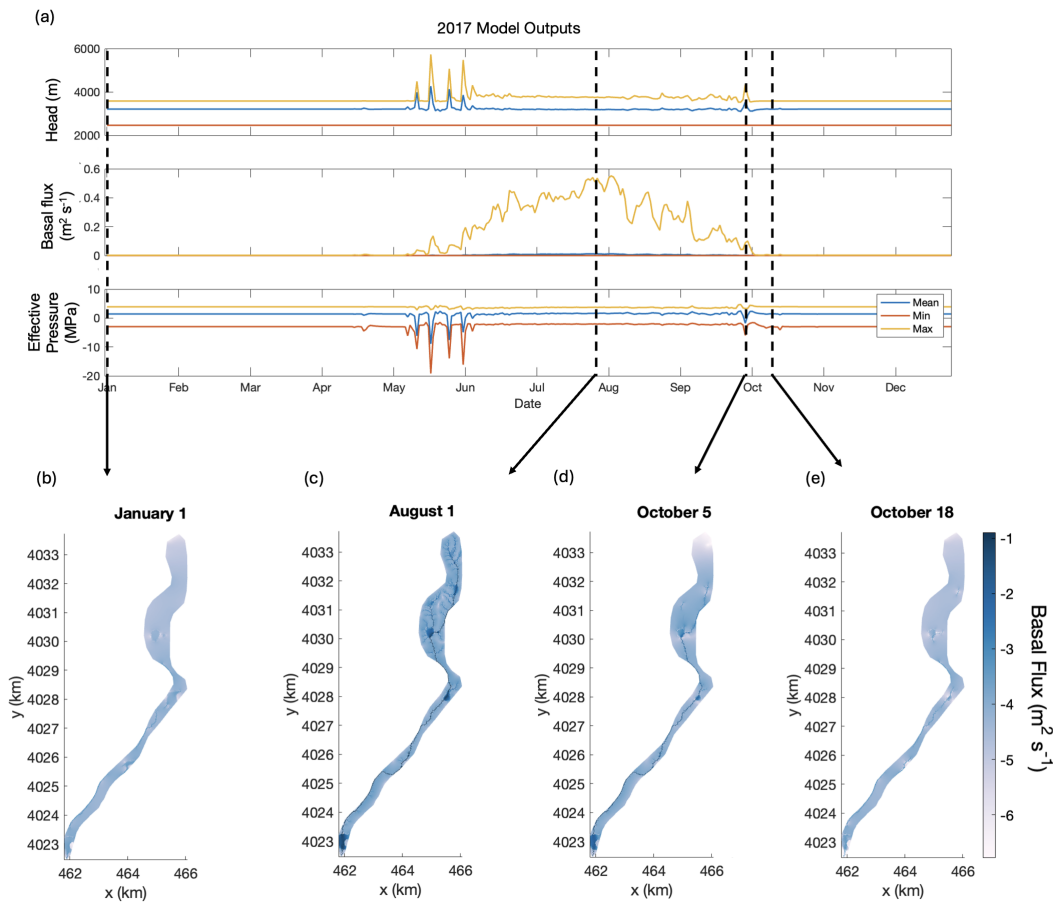


Fig. 4. (a) Model outputs for 2017 including hydraulic head, basal flux, and effective pressure. (b) Log_{10} basal flux across the glacier at four times during the year: January 1 (winter), August 1 (peak melt), October 5 (drawdown of drainage network at the end of the melt season), and October 18 (return to winter conditions).

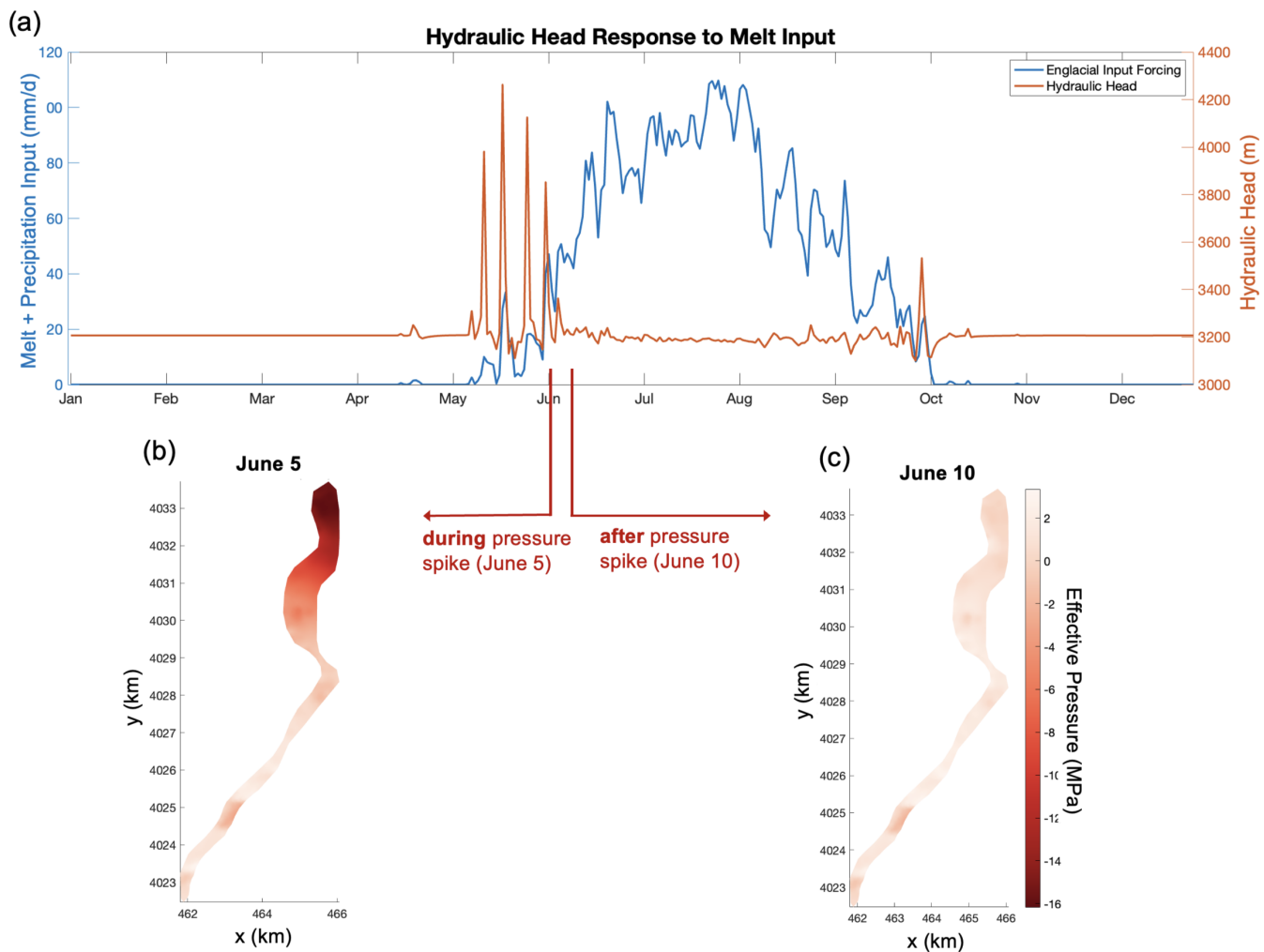


Fig. 5. Top: (a) Melt input (blue) overlaid with the model output hydraulic head (red) during 2017. Bottom: pressures across the mesh during (b) and after (c) the spike in hydraulic head in early June.

203 that this channel appears during the winter equilibration, during which time the only water at the ice-bed
 204 interface comes from pressure-induced melting and geothermal heat flux. Because Shishper is a temperate
 205 glacier, parts of the basal interface are usually able to be maintained at the pressure melting point for
 206 most of the year (Hubbard and Nienow, 1997). Therefore, there is always a consistent stream of water,
 207 although small, that keeps the main channel open. Bhambri and others (2020) show that surface melt
 208 elevations move from 6400 m in peak summer to 3500 m at the end of winter (no surface melt is observed
 209 in December, January, or February) meaning that the bottom part of the glacier will always receive more
 210 melt, and is more likely to contain channels, than the top.

211 Fig. 5 takes a closer look at the rapid decreases in effective pressure at the beginning of the melt season
 212 (May-July). Coming from distributed winter drainage, the rise in hydraulic head due to the system's

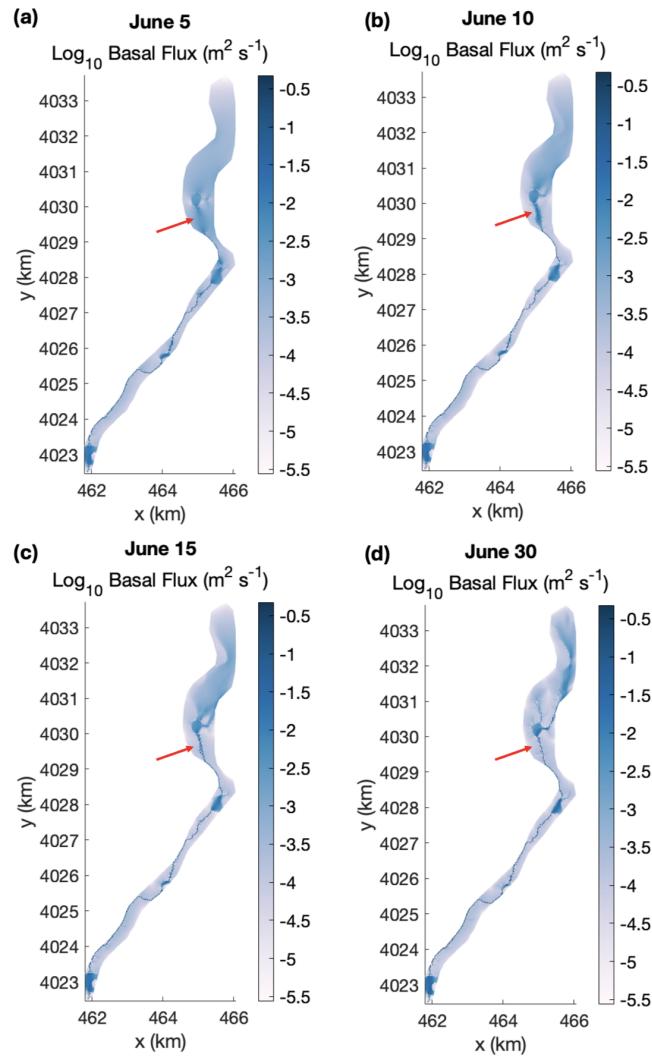


Fig. 6. Basal fluxes surrounding an early-season spike (depicted in Fig. 5) show a transition at the upper trunk from distributed, sheetlike flow to efficient, channelized flow.

213 inability to transport growing fluxes, and the rapid fall in head back to the equilibrium value shows that
 214 the system resolves this pressure by becoming more efficient. The buildup of hydraulic head can be observed
 215 in Fig. 5b (June 5), where a large area of negative N can be seen at the northern part of the domain.
 216 On June 10, this area of uplift at the northern part of the glacier has lessened, and by June 30 the entire
 217 section has almost completely returned to the original state of effective pressure, around 2 MPa across the
 218 mesh. Fig. 6 depicts the channel system that is established during and after these events, showing that
 219 an area of distributed, heavy flow around 4029 and 4030 km N quickly coalesces to a narrow and efficient
 220 channel in response to higher water pressures.

221 So long as high fluxes continue, melt opening exceeds creep closure, keeping channels open during

222 the majority of the melt season. The drainage system is able to quickly shuttle large fluxes through,
223 allowing it to return to a low-pressure state. Although velocities are not directly simulated here, it is likely
224 that sliding velocities decrease due to a return to higher effective pressures in the summer. Beaud and
225 others (2022)'s velocity dataset at Shishper Glacier from 2013-2019 shows that the glacier does indeed slow
226 down significantly during summer months. In addition, increases in surface displacement further up the
227 trunk of Shishper were observed by Bhambri and others (2020) during the early melt season (May to June)
228 between 2013-2016, indicating that there is decreased effective pressures at the northern part of the domain
229 during this time. This agrees with our model results: near the terminus, the system remains perennially
230 channelized, while the upper part sees an inefficient, distributed system during the early melt season.

231 As the system closes and the capacity of the drainage system falls, it re-gains its sensitivity to temporary
232 increases in melt, as is seen in the early and late summer spikes in hydraulic head (Fig. 5; Hart and others
233 (2022)). This contraction happens as basal flux falls, allowing melt opening to fall and creep closure to
234 dominate. The spikes are smaller than the ones at the beginning of the melt season because the system
235 has not had much time to close yet, so it is still more efficient than it would be at the beginning of spring.

236 Overall, these findings corroborate the established understanding that there is a transition from a
237 distributed to channelized drainage system and back during the course of the year (Fig. 4) (Schoof, 2010;
238 Werder and others, 2013; Flowers, 2015; Hubbard and Nienow, 1997). As long as high meltwater fluxes
239 persist, melt opening exceeds creep closure, maintaining open channels throughout most of the melt season
240 (Schoof, 2010; Werder and others, 2013; Flowers, 2015). As the system closes and the drainage capacity
241 decreases toward the end of the melt season, it regains sensitivity to temporary melt increases, which is
242 evident in early and late summer hydraulic head spikes (Fig. 5) (Bartholomew and others, 2012).

243 SHISHPER SURGE PHASES BETWEEN 2017 AND 2019

244 Hydrological Insights into Surge Dynamics

245 Comparing the modeled effective pressures with observed surge phases reveals that incipient surge motion
246 in November 2017 and subsequent slow acceleration through the winter 2017-2018 lack a clear hydrological
247 trigger, indicating a non-hydrological mechanism (Kamb, 1987; Björnsson, 1998). However, significant
248 hydraulic head spikes correspond with rapid acceleration in June 2018, suggesting that elevated water
249 pressures may have escalated already-occurring ice motion (Kamb, 1987; Björnsson, 1998).

250 Fig. 7 overlays effective pressure simulated by SHAKTI on top of satellite-derived velocity observations

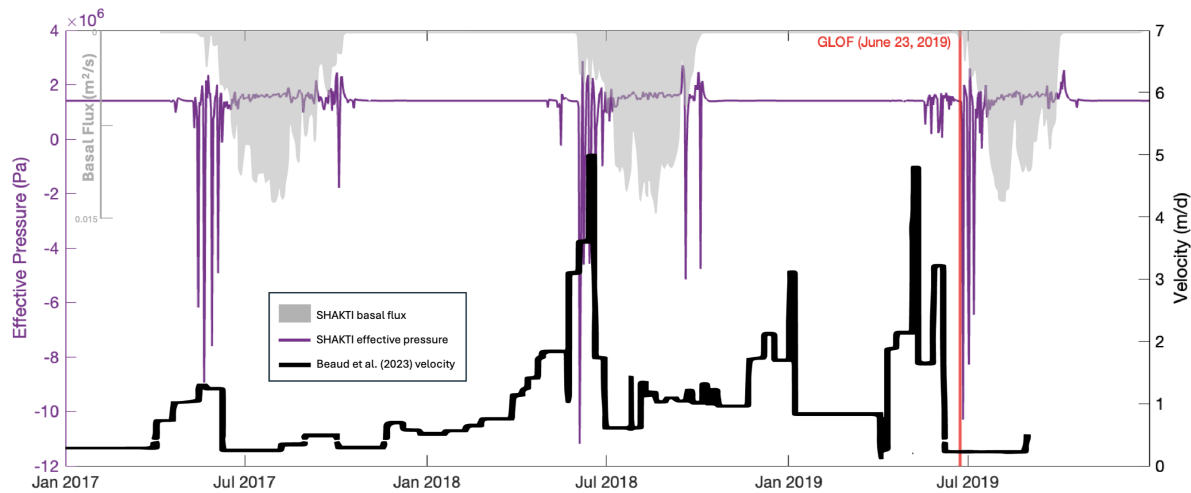


Fig. 7. Surge velocities from the dataset of Beaud and others (2022) overlaid on model outputs of head (m), basal flux (m^2/s) and effective pressure (Pa). The bright red line indicates a GLOF that occurred on June 22-23, 2019.

251 from Beaud and others (2022). Observations show a pre-surge acceleration begins in November 2017,
 252 but the model outputs indicate increase in subglacial lubrication during this acceleration (Kamb, 1987;
 253 Björnsson, 1998). At the beginning of June 2018, Bhambri and others (2020) describe a rapid but brief
 254 acceleration, which corresponds to the peak of about 5.5 m d^{-1} described by Beaud and others (2022)
 255 at the same time, coinciding with a series of modeled “spikes” in hydraulic head at the beginning of the
 256 2018 melt season. As the drainage system enters its efficient summer state, the surge then enters a very
 257 slow “semi-quiescent” period during which velocity is only slightly higher than normal summer velocities,
 258 lasting until September 2018 (Beaud and others, 2022). The glacier then accelerates again, reaching speeds
 259 of of approximately 2 m d^{-1} by November 2018 and 3.5 m d^{-1} in January 2019. Another surge peak occurs
 260 from late April to early May 2019 (Bhambri and others, 2020). A small GLOF of the proximal lake, which
 261 damaged the Karakoram Highway, follows from June 22-23, 2019 (Bhambri and others, 2020; Beaud and
 262 others, 2022).

263 Our simulated spring and fall dips in effective pressure correspond with Beaud and others (2022)’s
 264 observations of spring and fall speedups at Shishper Glacier even during quiescent (non-surgings) periods.
 265 The model results show larger and longer-duration effective pressure drops in spring compared to fall,
 266 aligning with observations of larger spring speedups. These findings support the hypotheses of observational
 267 studies suggesting that seasonal hydrology evolution is largely driving seasonal glacier motion trends in
 268 HMA (e.g., Nanni and others (2023); Sam and others (2018)).

269 Subglacial Hydrology's Contribution to Surge Motion

270 The slow acceleration to surge velocities beginning in November 2017 and continuing until January 2018
271 (Bhambri and others, 2020; Beaud and others, 2022) lacks a clear modeled hydrological trigger, indicating
272 a non-hydrological mechanism that is not accounted for by our model (Björnsson, 1998; Jiskoot and others,
273 2000). We suggest that some unknown factors(s) may first condition the glacier for surging, causing slow
274 acceleration - for example, a build-up of potential energy (i.e., through mass or enthalpy accumulation)
275 (Benn and others, 2019), dynamical thinning (i.e., as in Minchew and Meyer (2020)), or combination
276 of factors (Terleth and others, 2024) could put the system at an elevated state of surge "risk". Then, a
277 hydrological trigger could enhance ice velocities to sustain or set off additional surge motion. In our results,
278 spikes in hydraulic head corresponded to rapid acceleration in June 2018, suggesting that elevated water
279 pressures escalated the ice motion that was already occurring.

280 Role of Hydrology in Surge Termination

281 Subglacial hydrology may also or instead play a strong role in *halting* surge motion. Both surge peaks
282 ended when the system transitioned to a low pressure state (Fig. 7): the first in July 2018 after the
283 channelization of the early melt season and the second following a lake drainage in June 2019. The abrupt
284 transition from unstable, high water pressures to low (sub-flotation) pressures could play a significant role
285 in the termination of motion. Benn and others (2019) also found that in systems where surface water is
286 closely coupled to bed lubrication, surge motion terminates due to rapid discharge of water during the
287 switch from distributed to channelized drainage. Our findings, combined with those of Benn and others
288 (2019), support the idea that subglacial hydrology plays a stronger role in surge termination than initiation,
289 although it is important to note that the first channelization in spring 2018 did not completely stop surge
290 motion, as the channelization in 2019 did.

291 Why the surge terminated in 2019 (when the proximal lake drained through Shishper's terminus) but
292 not 2018, is unclear. The concurrent occurrence of surge termination and proximal lake drainages in the
293 Karakoram Range is well-established (e.g., Steiner and others (2018), Round and others (2017)). However,
294 the causal link between proximal lake drainage and surge termination requires further investigation.

295 **Limitations and Future Directions**

296 To further disentangle the drivers of surge motion, we need to consider and model additional processes such
297 as frictional feedbacks due to sliding at the ice-bed interface, till deformation, dynamic advances and retreat
298 of the terminus, and changes in ice thickness at the reservoir and receiving zone of the glacier. Two-way
299 coupling of SHAKTI with ice dynamics in ISSM has been implemented and applied recently to Helheim
300 Glacier, Greenland (Sommers and others, 2024), which could provide further insights into these complex
301 interactions. Future studies should focus on integrating these processes into the model to better understand
302 the interplay between subglacial hydrology, ice dynamics, proximal lake floods, and surge behavior.

303 **SUMMARY AND CONCLUSIONS**

304 Our study demonstrates that subglacial hydrology plays a crucial role in modulating glacier dynamics,
305 particularly in surge-type glaciers like Shishper. The simulations show that at least one year's melt cycle is
306 required to bring the drainage system to a long-term equilibrium in which the subglacial drainage system
307 returns to the same configuration every winter. This winter configuration features a single channel in the
308 lower trunk of the glacier which remains year-round and serves as the basis for an arborescent, channelized
309 drainage system that grows far up the glacier as the melt season peaks.

310 Our simulations also demonstrate SHAKTI's ability to represent the transition from an inefficient to
311 efficient drainage pattern as melt flux rises and vice versa. These transitions are marked by large spikes in
312 hydraulic head and corresponding dips in effective pressure, which support numerous previous observations
313 of spring and fall speedups at Shishper and other mountain glaciers and strengthen existing hypotheses
314 that seasonal glacier motion in High Mountain Asia is largely driven by changes in subglacial hydrology.

315 While subglacial hydrology may play a role in terminating surges or escalating an existing surge, it
316 cannot provide a standalone explanation for surge motion. The lack of a clear hydrological trigger for
317 incipient surge motion and for the second surge peak highlights the complexity of surge dynamics and the
318 need for further investigation into the interactions between subglacial hydrology, ice dynamics, and other
319 potential triggering mechanisms (Sevestre and Benn, 2015; Benn and others, 2019).

320 This is the first time the SHAKTI model has been applied to a realistic mountain glacier. While
321 our simulations here involve several simplifying assumptions, the successful reproduction of transitions
322 between distributed and channelized drainage over the course of several years provides a solid framework

323 for future work to refine the model. These future studies should focus on analyzing the complex coupling
324 between subglacial hydrology and glacier motion (Hoffman and Price, 2014; Sommers and others, 2024).
325 Additionally, investigating the causal link between proximal lake drainage and surge termination may
326 provide valuable insights into the role of subglacial hydrology in modulating surge behavior (Björnsson,
327 1998; Jiskoot and others, 2000).

328 ACKNOWLEDGEMENTS

329 We thank Flavien Beaud for his helpful advice and velocity dataset. We also thank Taylor Perron and
330 Camilla Cattania for their insightful feedback. This work was supported by the William Asbjornsen Albert
331 Memorial Fellowship and the MIT Office of Graduate Education. NN and WC also received support from
332 the Heising-Simons Foundation HSF-2020-1909.

333 Competing interests: The author(s) declare none.

334 REFERENCES

- 335 Anderson RS, Walder JS, Anderson SP, Trabant DC and Fountain AG (2005) The dynamic response of Kennicott
336 Glacier, Alaska, USA, to the Hidden Creek Lake outburst flood. *Annals of Glaciology*, **40**, 237–242, ISSN 0260-
337 3055, 1727-5644 (doi: 10.3189/172756405781813438)
- 338 Armstrong WH and Anderson RS (2020) Ice-marginal lake hydrology and the seasonal dynamical evolution
339 of Kennicott Glacier, Alaska. *Journal of Glaciology*, **66**(259), 699–713, ISSN 0022-1430, 1727-5652 (doi:
340 10.1017/jog.2020.41)
- 341 Bartholomew I, Nienow P, Sole A, Mair D, Cowton T and King MA (2012) Short-term variability in Greenland
342 Ice Sheet motion forced by time-varying meltwater drainage: Implications for the relationship between subglacial
343 drainage system behavior and ice velocity. *Journal of Geophysical Research: Earth Surface*, **117**(F3), ISSN 2156-
344 2202 (doi: 10.1029/2011JF002220), _eprint: <https://onlinelibrary.wiley.com/doi/pdf/10.1029/2011JF002220>
- 345 Bazai N, Cui P, Carling P, Wang H and Hassan J (2022a) Increasing the episodic glacial lake outburst flood hazard in
346 response to surge glaciers in the Karakoram. EGU22–752 (doi: 10.5194/egusphere-egu22-752), conference Name:
347 EGU General Assembly Conference Abstracts ADS Bibcode: 2022EGUGA..24..752B
- 348 Bazai NA, Cui P, Liu D, Carling PA, Wang H, Zhang G, Li Y and Hassan J (2022b) Glacier surging controls glacier
349 lake formation and outburst floods: The example of the Khurdopin Glacier, Karakoram. *Global and Planetary
350 Change*, **208**, 103710, ISSN 0921-8181 (doi: 10.1016/j.gloplacha.2021.103710)

- 351 Beaud F, Aati S, Delaney I, Adhikari S and Avouac JP (2021) Generalized sliding law applied to the surge dynamics
352 of Shisper Glacier and constrained by timeseries correlation of optical satellite images. preprint, *Glaciers/Remote*
353 *Sensing* (doi: 10.5194/tc-2021-96)
- 354 Beaud F, Aati S, Delaney I, Adhikari S and Avouac JP (2022) Surge dynamics of Shisper Glacier revealed by
355 time-series correlation of optical satellite images and their utility to substantiate a generalized sliding law. *The*
356 *Cryosphere*, **16**(8), 3123–3148, ISSN 1994-0416 (doi: 10.5194/tc-16-3123-2022), publisher: Copernicus GmbH
- 357 Benn DI, Fowler AC, Hewitt I and Sevestre H (2019) A general theory of glacier surges. *Journal of Glaciology*,
358 **65**(253), 701–716, ISSN 0022-1430, 1727-5652 (doi: 10.1017/jog.2019.62), publisher: Cambridge University Press
- 359 Bhambri R, Watson CS, Hewitt K, Haritashya UK, Kargel JS, Pratap Shahi A, Chand P, Kumar A, Verma A and
360 Govil H (2020) The hazardous 2017–2019 surge and river damming by Shispare Glacier, Karakoram. *Scientific*
361 *Reports*, **10**(1), 4685, ISSN 2045-2322 (doi: 10.1038/s41598-020-61277-8), number: 1 Publisher: Nature Publishing
362 Group
- 363 Bigelow DG, Flowers GE, Schoof CG, Mingo LDB, Young EM and Connal BG (2020) The Role of Englacial Hydrology
364 in the Filling and Drainage of an Ice-Dammed Lake, Kaskawulsh Glacier, Yukon, Canada. *Journal of Geophys-*
365 *ical Research: Earth Surface*, **125**(2), e2019JF005110, ISSN 2169-9011 (doi: 10.1029/2019JF005110), _eprint:
366 <https://onlinelibrary.wiley.com/doi/pdf/10.1029/2019JF005110>
- 367 Björnsson H (1998) Hydrological characteristics of the drainage system beneath a surging glacier. *Nature*, **395**(6704),
368 771–774, ISSN 1476-4687 (doi: 10.1038/27384), number: 6704 Publisher: Nature Publishing Group
- 369 Bolch T, Pieczonka T and Benn DI (2011) Multi-decadal mass loss of glaciers in the Everest area (Nepal Himalaya)
370 derived from stereo imagery. *The Cryosphere*, **5**(2), 349–358, ISSN 1994-0416 (doi: 10.5194/tc-5-349-2011), pub-
371 lisher: Copernicus GmbH
- 372 Braithwaite RJ (2008) Temperature and precipitation climate at the equilibrium-line altitude of glaciers expressed
373 by the degree-day factor for melting snow. *Journal of Glaciology*, **54**(186), 437–444, ISSN 0022-1430, 1727-5652
374 (doi: 10.3189/002214308785836968)
- 375 Copland L, Pope S, Bishop MP, John F Shroder J, Clendon P, Bush A, Kamp U, Seong YB and Owen LA (2009)
376 Glacier velocities across the central Karakoram. *Annals of Glaciology*, **50**(52), 41–49, ISSN 0260-3055, 1727-5644
377 (doi: 10.3189/172756409789624229)
- 378 Copland L, Sylvestre T, Bishop MP, Shroder JF, Seong YB, Owen LA, Bush A and Kamp U (2011) Expanded and
379 Recently Increased Glacier Surging in the Karakoram. *Arctic, Antarctic, and Alpine Research*, **43**(4), 503–516,
380 ISSN 1523-0430, 1938-4246 (doi: 10.1657/1938-4246-43.4.503)

- 381 Eisen O, Harrison WD and Raymond CF (2001) The surges of Variegated Glacier, Alaska, U.S.A., and their con-
382 nection to climate and mass balance. *Journal of Glaciology*, **47**(158), 351–358, ISSN 0022-1430, 1727-5652 (doi:
383 10.3189/172756501781832179), publisher: Cambridge University Press
- 384 Flowers G (2015) Modelling water flow under glaciers and ice sheets. *Proceedings of the Royal Society A: Mathematical,*
385 *Physical and Engineering Sciences*, **471** (doi: 10.1098/rspa.2014.0907)
- 386 Flowers GE, Björnsson H, Pálsson F and Clarke GKC (2004) A coupled sheet-conduit mechanism for jökulh-
387 laup propagation. *Geophysical Research Letters*, **31**(5), ISSN 1944-8007 (doi: 10.1029/2003GL019088), _eprint:
388 <https://onlinelibrary.wiley.com/doi/pdf/10.1029/2003GL019088>
- 389 Flowers GE, Roux N, Pimentel S and Schoof CG (2011) Present dynamics and future prognosis of a slowly surging
390 glacier. *The Cryosphere*, **5**(1), 299–313, ISSN 1994-0424 (doi: 10.5194/tc-5-299-2011)
- 391 German Aerospace Center (2018) TanDEM-X - Digital Elevation Model (DEM) - Global, 90m (doi:
392 10.15489/JU28HC7PUI09)
- 393 Gilbert A, Sinisalo A, Gurung TR, Fujita K, Maharjan SB, Sherpa TC and Fukuda T (2020) The influence of water
394 percolation through crevasses on the thermal regime of a Himalayan mountain glacier. *The Cryosphere*, **14**(4),
395 1273–1288, ISSN 1994-0416 (doi: 10.5194/tc-14-1273-2020), publisher: Copernicus GmbH
- 396 Gudmundsson MT, Björnsson H and Pálsson F (1995) Changes in jökulhlaup sizes in Grímsvötn, Vatnajökull, Iceland,
397 1934–91, deduced from in-situ measurements of subglacial lake volume. *Journal of Glaciology*, **41**(138), 263–272,
398 ISSN 0022-1430, 1727-5652 (doi: 10.3189/S0022143000016166), publisher: Cambridge University Press
- 399 Gulley J and Benn DI (2007) Structural control of englacial drainage systems in Himalayan debris-covered glaciers.
400 *Journal of Glaciology*, **53**(182), 399–412, ISSN 0022-1430, 1727-5652 (doi: 10.3189/002214307783258378)
- 401 Harrison S, Kargel JS, Huggel C, Reynolds J, Shugar DH, Betts RA, Emmer A, Glasser N, Haritashya UK, Klimeš
402 J, Reinhardt L, Schaub Y, Wiltshire A, Regmi D and Vilímek V (2018) Climate change and the global pattern of
403 moraine-dammed glacial lake outburst floods. *The Cryosphere*, **12**(4), 1195–1209, ISSN 1994-0416 (doi: 10.5194/tc-
404 12-1195-2018), publisher: Copernicus GmbH
- 405 Hart JK, Young DS, Baurley NR, Robson BA and Martinez K (2022) The seasonal evolution of subglacial drainage
406 pathways beneath a soft-bedded glacier. *Communications Earth & Environment*, **3**(1), 1–13, ISSN 2662-4435 (doi:
407 10.1038/s43247-022-00484-9), number: 1 Publisher: Nature Publishing Group
- 408 Hoffman M and Price S (2014) Feedbacks between coupled subglacial hydrology and glacier dynamics. *Journal of*
409 *Geophysical Research: Earth Surface*, **119**(3), 414–436, ISSN 2169-9011 (doi: 10.1002/2013JF002943), _eprint:
410 <https://onlinelibrary.wiley.com/doi/pdf/10.1002/2013JF002943>

- 411 Hubbard B and Nienow P (1997) Alpine subglacial hydrology. *Quaternary Science Reviews*, **16**(9), 939–955, ISSN
412 02773791 (doi: 10.1016/S0277-3791(97)00031-0)
- 413 Iken A and Bindschadler RA (1986) Combined measurements of Subglacial Water Pressure and Surface Velocity of
414 Findelengletscher, Switzerland: Conclusions about Drainage System and Sliding Mechanism. *Journal of Glaciol-*
415 *ogy*, **32**(110), 101–119, ISSN 0022-1430, 1727-5652 (doi: 10.3189/S0022143000006936), publisher: Cambridge
416 University Press
- 417 Iken A, Röthlisberger H, Flotron A and Haeberli W (1983) The Uplift of Unteraargletscher at the Beginning of
418 the Melt Season—A Consequence of Water Storage at the Bed? *Journal of Glaciology*, **29**(101), 28–47, ISSN
419 0022-1430, 1727-5652 (doi: 10.3189/S0022143000005128)
- 420 Jay-Allemand M, Gillet-Chaulet F, Gagliardini O and Nodet M (2011) Investigating changes in basal conditions of
421 Variegated Glacier prior to and during its 1982–1983 surge. *The Cryosphere*, **5**(3), 659–672, ISSN 1994-0416 (doi:
422 10.5194/tc-5-659-2011), publisher: Copernicus GmbH
- 423 Jiskoot H, Murray T and Boyle P (2000) Controls on the distribution of surge-type glaciers in Svalbard. *Jour-*
424 *nal of Glaciology*, **46**(154), 412–422, ISSN 0022-1430, 1727-5652 (doi: 10.3189/172756500781833115), publisher:
425 Cambridge University Press
- 426 Kamb B (1987) Glacier surge mechanism based on linked cavity configuration of the basal water conduit system.
427 *Journal of Geophysical Research*, **92**(B9), 9083, ISSN 0148-0227 (doi: 10.1029/JB092iB09p09083)
- 428 Kingslake J and Ng F (2013) Modelling the coupling of flood discharge with glacier flow during jökulhlaups. *Annals*
429 *of Glaciology*, **54**(63), 25–31, ISSN 0260-3055, 1727-5644 (doi: 10.3189/2013AoG63A331)
- 430 Kusch E and Davy R (2022) KrigR—a tool for downloading and statistically downscaling climate reanalysis data.
431 *Environmental Research Letters*, **17**(2), 024005, ISSN 1748-9326 (doi: 10.1088/1748-9326/ac48b3), publisher: IOP
432 Publishing
- 433 Larour E, Seroussi H, Morlighem M and Rignot E (2012) Continental scale, high order, high spa-
434 tial resolution, ice sheet modeling using the Ice Sheet System Model (ISSM). *Journal of Geo-*
435 *physical Research: Earth Surface*, **117**(F1), ISSN 2156-2202 (doi: 10.1029/2011JF002140), _eprint:
436 <https://onlinelibrary.wiley.com/doi/pdf/10.1029/2011JF002140>
- 437 Litt M, Shea J, Wagnon P, Steiner J, Koch I, Stigter E and Immerzeel W (2019) Glacier ablation and temperature in-
438 dexed melt models in the Nepalese Himalaya. *Scientific Reports*, **9**(1), 5264, ISSN 2045-2322 (doi: 10.1038/s41598-
439 019-41657-5), number: 1 Publisher: Nature Publishing Group

- 440 Liu J, Enderlin EM, Bartholomaus TC, Terleth Y, Mikesell TD and Beaud F (2024) Propagating speedups during
441 quiescence escalate to the 2020–2021 surge of Sít' Kusá, southeast Alaska. *Journal of Glaciology*, 1–12, ISSN
442 0022-1430, 1727-5652 (doi: 10.1017/jog.2023.99), publisher: Cambridge University Press
- 443 Miles ES, Steiner J, Willis I, Buri P, Immerzeel WW, Chesnokova A and Pellicciotti F (2017) Pond Dynamics and
444 Supraglacial-Englacial Connectivity on Debris-Covered Lirung Glacier, Nepal. *Frontiers in Earth Science*, **5**, ISSN
445 2296-6463 (doi: 10.3389/feart.2017.00069), publisher: Frontiers
- 446 Miles KE, Hubbard B, Quincey DJ, Miles ES, Irvine-Fynn TD and Rowan AV (2019) Surface and subsurface hydrology
447 of debris-covered Khumbu Glacier, Nepal, revealed by dye tracing. *Earth and Planetary Science Letters*, **513**, 176–
448 186, ISSN 0012821X (doi: 10.1016/j.epsl.2019.02.020)
- 449 Miles KE, Hubbard B, Miles ES, Quincey DJ, Rowan AV, Kirkbride M and Hornsey J (2021) Continuous borehole
450 optical televising reveals variable englacial debris concentrations at Khumbu Glacier, Nepal. *Communications
451 Earth & Environment*, **2**(1), 1–9, ISSN 2662-4435 (doi: 10.1038/s43247-020-00070-x), publisher: Nature Publishing
452 Group
- 453 Millan R, Mouginot J, Rabatel A and Morlighem M (2022) Ice velocity and thickness of the world's glaciers. *Nature
454 Geoscience*, **15**(2), 124–129, ISSN 1752-0908 (doi: 10.1038/s41561-021-00885-z), number: 2 Publisher: Nature
455 Publishing Group
- 456 Minchew B, Simons M, Björnsson H, Pálsson F, Morlighem M, Seroussi H, Larour E and Hensley S (2016) Plastic
457 bed beneath Hofsjökull Ice Cap, central Iceland, and the sensitivity of ice flow to surface meltwater flux. *Journal
458 of Glaciology*, **62**(231), 147–158, ISSN 0022-1430, 1727-5652 (doi: 10.1017/jog.2016.26), publisher: Cambridge
459 University Press
- 460 Minchew BM and Meyer CR (2020) Dilation of subglacial sediment governs incipient surge motion in glaciers with
461 deformable beds. *Proceedings of the Royal Society A: Mathematical, Physical and Engineering Sciences*, **476**(2238),
462 20200033 (doi: 10.1098/rspa.2020.0033), publisher: Royal Society
- 463 Muhammad S, Li J, Steiner JF, Shrestha F, Shah GM, Berthier E, Guo L, Wu Lx and Tian L (2021) A holistic view
464 of Shisper Glacier surge and outburst floods: from physical processes to downstream impacts. *Geomatics, Natural
465 Hazards and Risk*, **12**(1), 2755–2775, ISSN 1947-5705 (doi: 10.1080/19475705.2021.1975833), publisher: Taylor &
466 Francis _eprint: <https://doi.org/10.1080/19475705.2021.1975833>
- 467 Murray T, Stuart GW, Miller PJ, Woodward J, Smith AM, Porter PR and Jiskoot H (2000) Glacier surge propagation
468 by thermal evolution at the bed. *Journal of Geophysical Research: Solid Earth*, **105**(B6), 13491–13507, ISSN 2156-
469 2202 (doi: 10.1029/2000JB900066), _eprint: <https://onlinelibrary.wiley.com/doi/pdf/10.1029/2000JB900066>

- 470 Muñoz-Sabater J, Dutra E, Agustí-Panareda A, Albergel C, Arduini G, Balsamo G, Boussetta S, Choulga M, Harrigan
471 S, Hersbach H, Martens B, Miralles DG, Piles M, Rodríguez-Fernández NJ, Zsoter E, Buontempo C and Thépaut
472 JN (2021) ERA5-Land: a state-of-the-art global reanalysis dataset for land applications. *Earth System Science
473 Data*, **13**(9), 4349–4383, ISSN 1866-3508 (doi: 10.5194/essd-13-4349-2021), publisher: Copernicus GmbH
- 474 Nanni U, Scherler D, Ayoub F, Millan R, Herman F and Avouac JP (2023) Climatic control on seasonal variations
475 in mountain glacier surface velocity. *The Cryosphere*, **17**(4), 1567–1583, ISSN 1994-0416 (doi: 10.5194/tc-17-1567-
476 2023), publisher: Copernicus GmbH
- 477 Nienow PW, Hubbard AL, Hubbard BP, Chandler DM, Mair DWF, Sharp MJ and Willis IC
478 (2005) Hydrological controls on diurnal ice flow variability in valley glaciers. *Journal of Geo-
479 physical Research: Earth Surface*, **110**(F4), ISSN 2156-2202 (doi: 10.1029/2003JF000112), _eprint:
480 <https://onlinelibrary.wiley.com/doi/pdf/10.1029/2003JF000112>
- 481 Nye JF (1976) Water Flow in Glaciers: Jökulhlaups, Tunnels and Veins. *Journal of Glaciology*, **17**(76), 181–207,
482 ISSN 0022-1430, 1727-5652 (doi: 10.3189/S002214300001354X), publisher: Cambridge University Press
- 483 Pritchard HD, King EC, Goodger DJ, McCarthy M, Mayer C and Kayastha R (2020) Towards Bedmap Himalayas:
484 development of an airborne ice-sounding radar for glacier thickness surveys in High-Mountain Asia. *Annals of
485 Glaciology*, **61**(81), 35–45, ISSN 0260-3055, 1727-5644 (doi: 10.1017/aog.2020.29)
- 486 RGI Consortium (2017) Randolph glacier inventory - a dataset of global glacier outlines, version 6 (doi:
487 10.7265/4M1F-GD79)
- 488 Rounce DR, Hock R and Shean DE (2020) Glacier Mass Change in High Mountain Asia Through 2100 Using the
489 Open-Source Python Glacier Evolution Model (PyGEM). *Frontiers in Earth Science*, **7**, ISSN 2296-6463
- 490 Round V, Leinss S, Huss M, Haemmig C and Hajnsek I (2017) Surge dynamics and lake outbursts of Kyagar
491 Glacier, Karakoram. *The Cryosphere*, **11**(2), 723–739, ISSN 1994-0416 (doi: 10.5194/tc-11-723-2017), publisher:
492 Copernicus GmbH
- 493 Röthlisberger H (1972) Water Pressure in Intra- and Subglacial Channels. *Journal of Glaciology*, **11**(62), 177–203,
494 ISSN 0022-1430, 1727-5652 (doi: 10.3189/S0022143000022188), publisher: Cambridge University Press
- 495 Sam L, Bhardwaj A, Kumar R, Buchroithner MF and Martín-Torres FJ (2018) Heterogeneity in topographic control
496 on velocities of Western Himalayan glaciers. *Scientific Reports*, **8**(1), 12843, ISSN 2045-2322 (doi: 10.1038/s41598-
497 018-31310-y)
- 498 Schoof C (2010) Ice-sheet acceleration driven by melt supply variability. *Nature*, **468**(7325), 803–806, ISSN 1476-4687
499 (doi: 10.1038/nature09618), number: 7325 Publisher: Nature Publishing Group

- Scott CA, Zhang F, Mukherji A, Immerzeel W, Mustafa D and Bharati L (2019) Water in the Hindu Kush Himalaya. In P Wester, A Mishra, A Mukherji and AB Shrestha (eds.), *The Hindu Kush Himalaya Assessment: Mountains, Climate Change, Sustainability and People*, 257–299, Springer International Publishing, Cham, ISBN 978-3-319-92288-1 (doi: 10.1007/978-3-319-92288-1₈)
- 500 Setchell H (2020) ECMWF Reanalysis v5
- 501 Sevestre H and Benn DI (2015) Climatic and geometric controls on the global distribution of surge-type glaciers: implications for a unifying model of surging. *Journal of Glaciology*, **61**(228), 646–662, ISSN 0022-1430, 1727-5652 (doi: 10.3189/2015JoG14J136), publisher: Cambridge University Press
- 502
503
- 504 Shean DE, Bhushan S, Montesano P, Rounce DR, Arendt A and Osmanoglu B (2020) A Systematic, Regional Assessment of High Mountain Asia Glacier Mass Balance. *Frontiers in Earth Science*, **7**, ISSN 2296-6463 (doi: 10.3389/feart.2019.00363), publisher: Frontiers
- 505
506
- 507 Shepherd A, Hubbard A, Nienow P, King M, McMillan M and Joughin I (2009) Greenland ice sheet motion coupled with daily melting in late summer. *Geophysical Research Letters*, **36**(1), ISSN 1944-8007 (doi: 10.1029/2008GL035758),
508
509 __eprint: <https://onlinelibrary.wiley.com/doi/pdf/10.1029/2008GL035758>
- 510 Shrestha F, Steiner JF, Shrestha R, Dhungel Y, Joshi SP, Inglis S, Ashraf A, Wali S, Walizada KM and Zhang T (2023) A comprehensive and version-controlled database of glacial lake outburst floods in High Mountain Asia. *Earth System Science Data*, **15**(9), 3941–3961, ISSN 1866-3508 (doi: 10.5194/essd-15-3941-2023), publisher: Copernicus
511
512
513 GmbH
- 514 Sommers A, Rajaram H and Morlighem M (2018) SHAKTI: Subglacial Hydrology and Kinetic, Transient Interactions v1.0. *Geoscientific Model Development*, **11**(7), 2955–2974, ISSN 1991-959X (doi: 10.5194/gmd-11-2955-2018),
515
516 publisher: Copernicus GmbH
- 517 Sommers AN, Meyer CR, Poinar K, Mejia J, Morlighem M, Rajaram H, Warburton KLP and Chu W (2024) Velocity of Greenland's Helheim Glacier Controlled Both by Terminus Effects and Subglacial Hydrology With Distinct Realms of Influence. *Geophysical Research Letters*, **51**(15), e2024GL109168, ISSN 1944-8007 (doi: 10.1029/2024GL109168),
518
519 __eprint: <https://onlinelibrary.wiley.com/doi/pdf/10.1029/2024GL109168>
- 520
- 521 Steiner JF, Kraaijenbrink PDA, Jiduc SG and Immerzeel WW (2018) Brief communication: The Khurdopin glacier surge revisited – extreme flow velocities and formation of a dammed lake in 2017. *The Cryosphere*, **12**(1), 95–101, ISSN 1994-0416 (doi: 10.5194/tc-12-95-2018), publisher: Copernicus GmbH
522
523
- 524 Terleth Y, Bartholomaus TC, Enderlin E, Mikesell TD and Liu J (2024) Glacier Surges and Seasonal Speedups Integrated Into a Single, Enthalpy-Based Model Framework. *Geophysical Research Letters*, **51**(23), e2024GL112514, ISSN 1944-8007 (doi: 10.1029/2024GL112514), __eprint: <https://onlinelibrary.wiley.com/doi/pdf/10.1029/2024GL112514>
525
526

527Werder MA, Hewitt IJ, Schoof CG and Flowers GE (2013) Modeling channelized and distributed subglacial drainage
528 in two dimensions: A 2-D SUBGLACIAL DRAINAGE SYSTEM MODEL. *Journal of Geophysical Research: Earth*
529 *Surface*, **118**(4), 2140–2158, ISSN 21699003 (doi: 10.1002/jgrf.20146)

530Zhang G, Bolch T, Yao T, Rounce DR, Chen W, Veh G, King O, Allen SK, Wang M and Wang W (2023a) Underes-
531 timated mass loss from lake-terminating glaciers in the greater Himalaya. *Nature Geoscience*, **16**(4), 333–338, ISSN
532 1752-0908 (doi: 10.1038/s41561-023-01150-1), publisher: Nature Publishing Group

533Zhang G, Carrivick JL, Emmer A, Shugar DH, Veh G, Wang X, Labeledz C, Mergili M, Mölg N, Huss M, Allen S,
534 Sugiyama S and Lützow N (2024) Characteristics and changes of glacial lakes and outburst floods. *Nature Reviews*
535 *Earth & Environment*, 1–16, ISSN 2662-138X (doi: 10.1038/s43017-024-00554-w), publisher: Nature Publishing
536 Group

537Zhang T, Wang W, An B and Wei L (2023b) Enhanced glacial lake activity threatens numerous communities and
538 infrastructure in the Third Pole. *Nature Communications*, **14**(1), 8250, ISSN 2041-1723 (doi: 10.1038/s41467-023-
539 44123-z), number: 1 Publisher: Nature Publishing Group

540Zheng G, Allen SK, Bao A, Ballesteros-Cánovas JA, Huss M, Zhang G, Li J, Yuan Y, Jiang L, Yu T, Chen W and
541 Stoffel M (2021) Increasing risk of glacial lake outburst floods from future Third Pole deglaciation. *Nature Climate*
542 *Change*, **11**(5), 411–417, ISSN 1758-6798 (doi: 10.1038/s41558-021-01028-3), publisher: Nature Publishing Group

543Zwally J, Abdalati W, Herring T, Larsen K, Saba J and Steffen K (2002) Surface Melt-Induced Acceleration of Greenland
544 Ice-Sheet Flow. *Science*, **297**(5579) (doi: 10.1126/science.1072708)

545 **APPENDIX A: MESH RESOLUTION TESTS**

546 We conducted a simple test of the finite element mesh resolution to ensure that the development of basal
547 channels was not dependent on an arbitrary choice of mesh element size. We ran winter equilibrations
548 with triangular mesh sizes of 10m, 20m, 40m, 50m, 100m, 200m, and 250m. Each was run with 6-hour
549 timesteps for 300 days and were initialized with the same initial conditions. In Fig. 8 we show gap heights
550 at the end of each of these winter equilibrations.

551 Areas of high gap height show the location of channels and subglacial lakes. The location of these chan-
552 nels is largely invariant with mesh resolution, suggesting that channel locations exhibit a higher dependence
553 on topography than on mesh resolution.

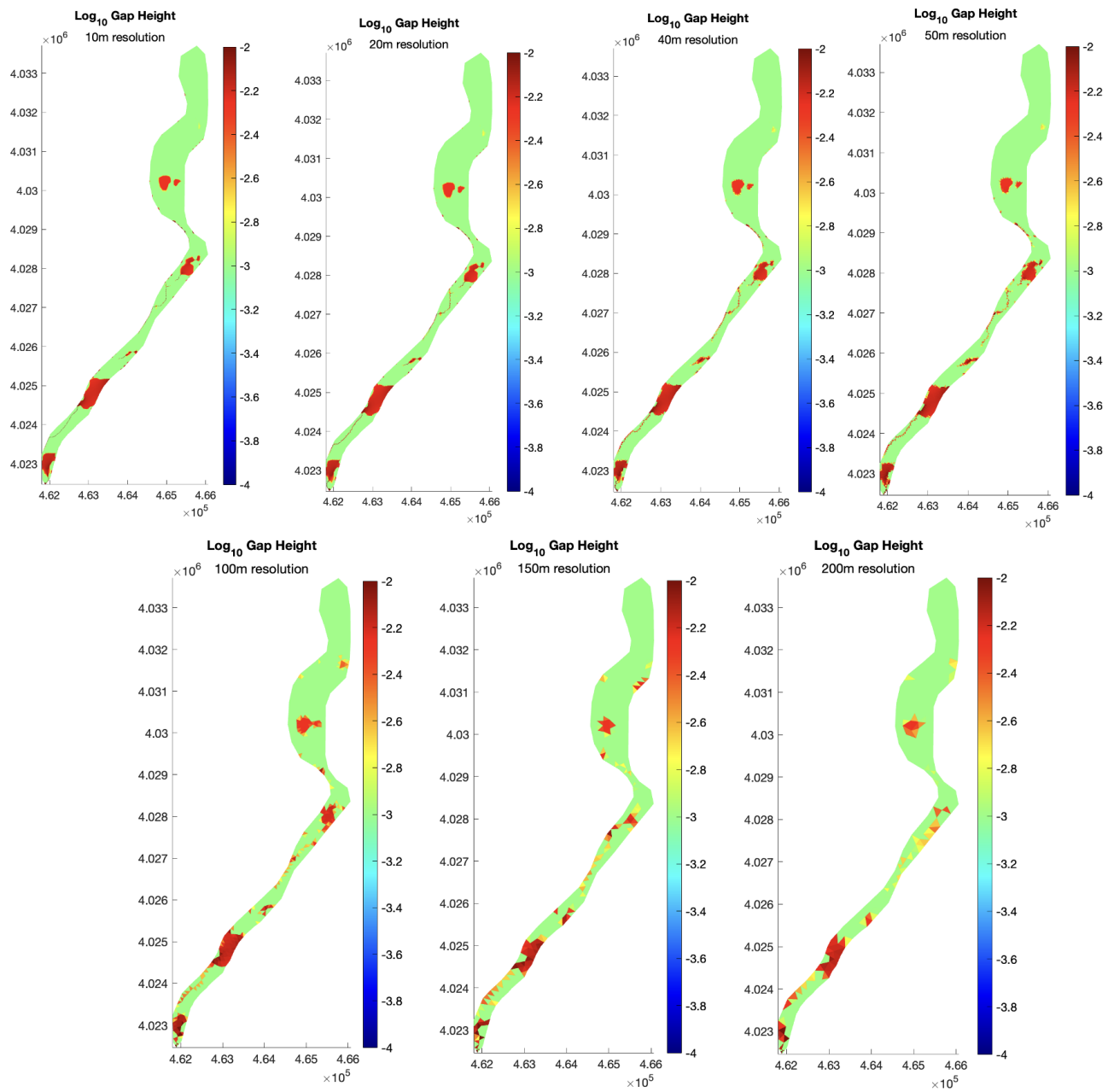


Fig. 8. Gap height (m) across the domain, shown for mesh resolutions of 10 m, 20 m, 40 m, 50 m, 100 m, 150 m, and 200 m.